Rock characteristics of post-caldera volcanoes in Dieng volcanic complex (DVC), Central Java, Indonesia

Indranova Suhendro [1]*, Muhammad Nadafa Isnain[1], Rizky Wahyudi[1]

[1] *Department of Environmental Geography, Faculty of Geography, Universitas Gadjah Mada, Sekip Utara Jl. Kaliurang, Bulaksumur, Yogyakarta, 55281, Indonesia*

* Corresponding author : indranova.suhendro@mail.ugm.ac.id
Tel.:+62-889-526-3638

Abstract

The Dieng volcanic complex (DVC) has one of the densest post-caldera volcanisms activity presents in Indonesia, yet its population density is considerably high. Therefore, it is important to identify the rock characteristics produced by the DVC post-caldera volcanoes to understand the risks and future hazards (i.e., eruption style). Based on lithology, we have classified DVC post-caldera volcanoes as (1) pyroclastic domain (PD; including Pagerkandang, Merdada, and Pangonan), and (2) lava domain (LD; including Prambanan, Kendil, Pakuwaja, Sikunir, Sikarim, and Seroja). PD is characterized by the domination of pyroclastic materials (mostly ash and lapilli) with oxidized scoria and volcanic lithics (fresh and/or altered) as the main components. The oxidized scoria clasts are moderately vesicular (27–41 % vesicularity; ϕ_V) and phenocryst poor (<5 % phenocryst crystallinity, ϕ_{PC}), with plagioclase, pyroxene, and oxides as the main phenocryst phases. The LD is composed predominantly of lava. The observed lavas are typically dense (mostly <1 % ϕ_V), phenocryst rich (21–47 % ϕ_{PC}), and include plagioclase, pyroxene, biotite, amphibole, and oxides as the main phenocryst phases. Such differences in mineralogy and textures (i.e., vesicularity and crystallinity) suggest that PD and LD were likely sourced from different magmatic sources with different eruption styles (explosive and effusive styles, respectively). We have suggested that civilization settlements near PD are facing major threats from explosive magmatic, phreatomagmatic, and phreatic eruptions that could produce significant fallouts, ballistic materials, and highly destructive pyroclastic density currents. LDs pose a threat in the form of effusive magmatic eruptions such as lava flows and/or domes.

Keywords: Dieng Volcanic Complex, Post-Caldera Volcanism, Lava, Pyroclastic Rocks, Eruption

1. Introduction

Post-caldera volcanism is known to reflect active magmatic conditions after the collapse of a volcanic edifice (Sigurdsson, 2000). Such processes might occur through (1) centralized vents (e.g., Sakurajima in the Aira caldera, Barujari in the Samalas caldera, and Batur in the Batur caldera; Araya et al., 2019; Rachmat et al., 2016; Reubi and Nicholls, 2004) and/or (2) random-scattered vents in the inner and rim of a caldera (e.g., Aniakchak, Dieng, and Ijen volcanic complexes; Browne et al., 2022; Harijoko et al., 2016; Suhendro, 2016). In the first type, predicting future eruptions may be relatively easy because the magma extrusion takes place from centralized vent(s) (Araya et al. 2019; Rachmat et al. 2016; Rubin' et al. 1989). However, predicting future eruptions from the second type may be very challenging owing to the uncertainty of the vent(s) location. It is therefore important to identify the pattern and behavior of the second type of post-caldera volcanism (including the eruption style, deposition characteristics, and stratigraphy) to gain a better understanding of its eruption dynamics, which can be utilized as a basis for hazard assessment. To shed light on this issue, we have studied the post-caldera volcanoes of Dieng volcanic complex (DVC) in Central Java, Indonesia (Fig. 1a, b). We selected this area for our study for two main reasons: (1) Dieng is known as a volcanic complex that hosts one of the densest post-caldera volcanisms activity in Indonesia (there are approximately nine post-caldera volcanoes occupying the inner caldera (ca. area of ±40 km^2)), and (2) the DVC is a home of abundant civilization settlements (approximately 1794 people/km^2) (Badan Pusat

Statistik Kabupaten Wonosobo 2020). This has become more serious because there are many settlements situated very close (less than 200 m) to the active craters, such as Sileri, Sinila, and Sikidang. Moreover, the phreatic eruption of the Sinila crater in 1979 has shown us how dangerous a post-caldera volcano can be, even without any magma extrusions (the eruption released a CO_2-dominated gas and killed 142 people; le Guern et al., 1982).

Herein, we report the results of fieldwork on nine post-caldera volcanoes in the DVC, namely Sikunir, Seroja, Pakuwaja, Sikarim, Kendil, Prambanan, Pangonan, Merdada, and Pagerkandang (Fig. 1b). These fieldwork results were then combined with qualitative morphometric observations to produce a geological map of the study area.

Subsequently, we have then reported the results of quantitative analyses of the grain size distribution (GSD), componentry, phenocrysts (modal mineralogy and phenocryst content), and vesicles (bulk vesicularity and vesicle number density). However, GSD and componentry analyses can only be performed for pyroclastic materials. In addition, we have reported the chemical composition of the scoria clast groundmass glass. Finally, quantitative and chemical analyses were performed to understand the eruption dynamics of the DVC post-caldera volcanoes. We suggest that syn-eruptive processes (degassing and decompression rate) coupled with external factors (i.e., groundwater and lake) play an important role in controlling the eruption style (effusive or explosive), and ultimately, the future hazards that can possibly occur (i.e., lava

flows, lava domes, pyroclastic fallouts, pyroclastic density currents (PDCs)).
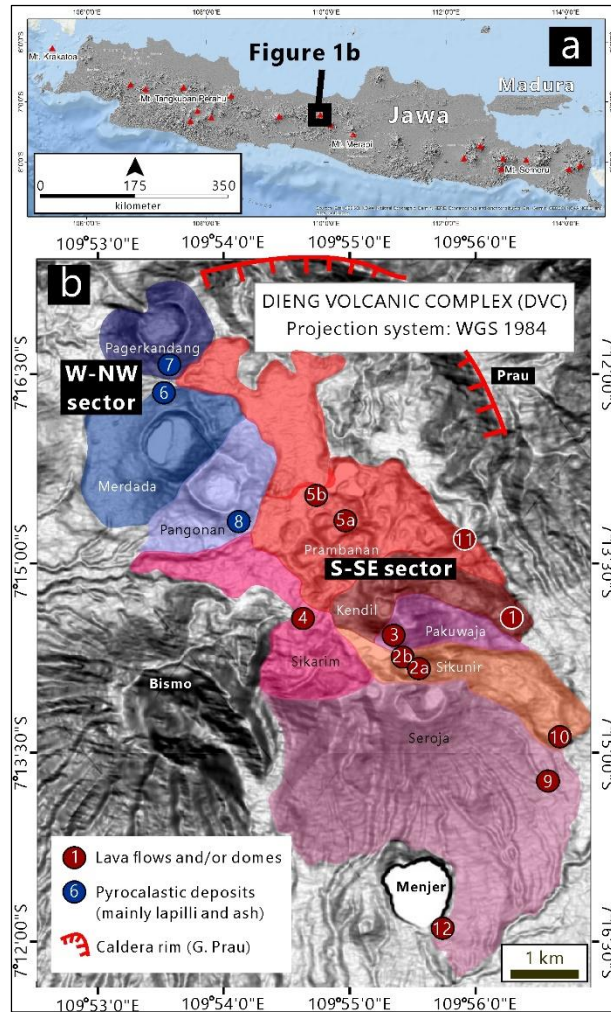
Fig. 1. (a) Location of Dieng volcanic complex (DVC). (b) Map showing the distribution of our sampling locations. Red circle denotes lava flows and/or domes, while blue circle represents pyroclastic deposits. Data source of the topographic map: Badan Informasi Geospasial, 2018. Note that PD volcanoes are typically having large crater sizes compared to LD volcanoes.
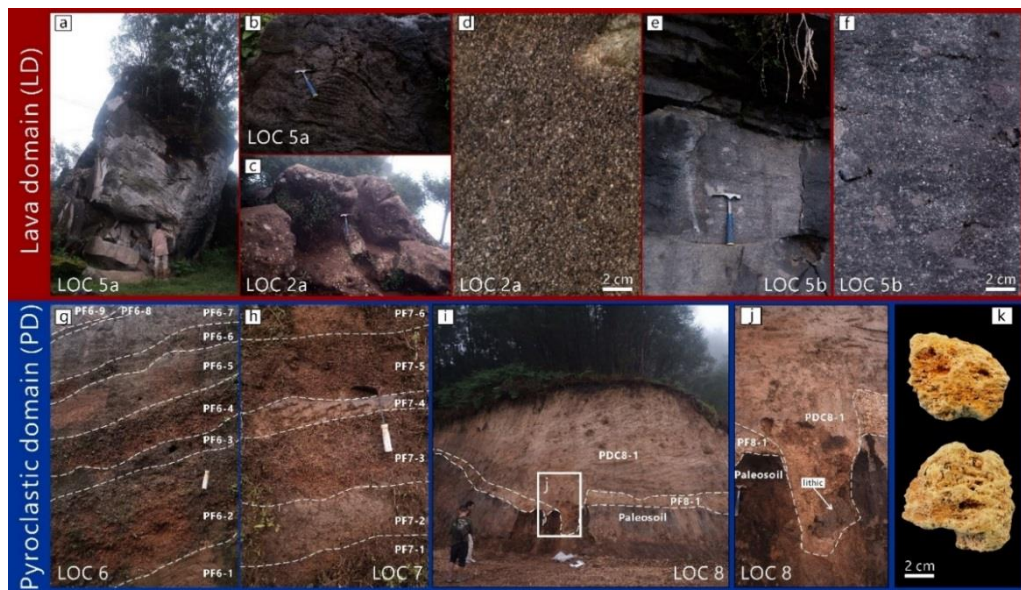
Fig. 2. Lavas in the proximal zone (vent area) shows foliation (a), flow-banding structure (b), brecciation (c), with abundant phenocryst content (d). Distal lavas are typically massive (with minor sheeting joints) and contain less abundant phenocryst content than the proximal lavas (e, f). Intercalation of ash and lapilli falls from Pagerkandang (g) and Merdada (h). By contrast, Pangonan shows a relatively simpler stratigraphic section than the later, as there are only two pyroclastic layers (PF 8-1 and PDC 8-1) above the paleosoil (i). Bomb sag of large lithic clasts cause the discontinuity of PF 8-1 and PDC 8-1 layers (j). Representative images of oxidized scoria clasts (k)
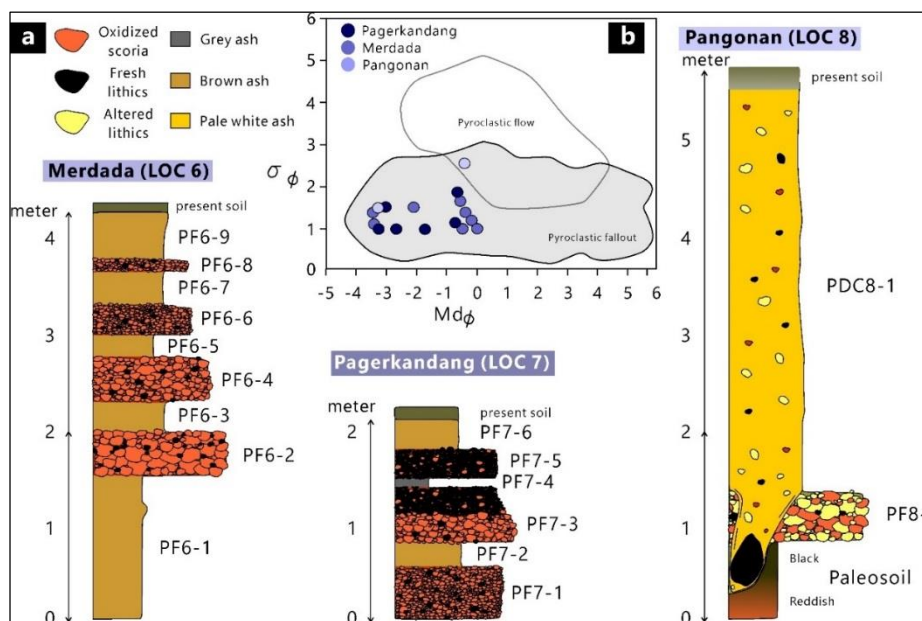
Fig. 3. (a) Stratigraphic column of Merdada, Pagerkandang, and Pangonan. (b) Deposits of Pagerkandang and Merdada were resulted from pyroclastic fall, while Pangonan comprise of pyroclastic fall and pyroclastic density current (flow).

2. Dieng Volcanic Complex (DVC)

The Dieng volcanic complex (DVC) is a Quaternary volcano in Central Java, Indonesia (Fig. 1a) (Harijoko et al. 2016). Its caldera structure has a circular depression which extend from the northern to the eastern side of the DVC (Gunung Prau, Fig. 1b). Although the DVC is thought to have experienced a caldera formation process (Sukhyar et al., 1986), such fundamental information on its caldera-forming eruption deposits is still lacking (i.e., a thick sequence of pumice and/or scoria fall and ignimbrite deposits). This may be caused by intense post-caldera volcano activities, as the deposition of younger volcanic products will bury the older deposits.

Sukhyar et al. (1986) classified DVC rocks into the categories of pre-collapse, second, and youngest episodes. The oldest group (pre-collapse episode) is represented by the rocks from Gunung Prau with an estimated age of 1.1±0.9 Ma (Harijoko et al. 2016). This group covers a narrow variation in the bulk-rock chemical compositions (basalt to basaltic andesite, (±49–57 wt. % SiO_2) with phenocryst variations of plagioclase (Pl), clinopyroxene (Cpx), orthopyroxene (Opx), olivine (Ol), and oxides (Ox) (Harijoko et al. 2015). The second episode was represented by rocks from Pagerkandang, Bucu, and Pangonan-Merdada, with the magma compositions ranging from basalt to andesite (±51.6–63.1 wt. % SiO_2) (Harijoko et al. 2016). However, there have been no reports on the mineral assemblages in the second episode. Based on K-Ar analysis, the age of second episode group is found to be 0.46–0.37 Ma (Harijoko et al. 2016). The youngest episode represents the youngest and most evolved rocks in DVC (±0.27–0.07 Ma and 59.6–64.5 wt. % SiO_2, respectively), with plagioclase as the most abundant mineral phase, followed by clinopyroxene, orthopyroxene, biotite, amphibole, and various oxides. It is worth noting that there is a tendency of increasing silica content from the pre-caldera to the youngest episodes (Harijoko et al. 2016). Such evidence coupled with the fact that hydrous minerals (i.e., biotite and amphibole) only exist in the youngest episode suggests that the DVC has experienced an intensive fractional crystallization process.

3. Fieldwork

In general, post-caldera volcanism in the DVC displays typical distinctive rock types between the south and -southeast

(S-SE) and west-northwest (W-NW) sectors. In particular, the S-SE sector (Sikunir, Seroja, Pakuwaja, Sikarim, Kendil, and Prambanan) is dominated by lava flows and/or domes, whereas the W-NW sector (Pangonan, Merdada, Pagerkandang) is predominantly composed of pyroclastic materials (Fig. 1b). Hereafter, we consider the S-SE and W-NW sector post-caldera volcanoes as the lava domain (LD) and pyroclastic domain (PD), respectively.

The LD outcrops are typically thick (up to several tens meters), massive, intensively fractured, and phenocryst-rich (Fig. 2a-f). Some may display foliations (Fig. 2a) and flow-banding structures (Fig. 2b), but they are exclusive to the proximal zone (vent area). It is worth noting that proximal lava outcrops tended to have higher phenocryst content than distal lava (Fig. 2d and f). The PD outcrops are characterized by the stratification of pyroclastic materials (mostly ash and lapilli; Fig. 2g-j). In particular, we have identified (at least) nine, six, and two main tephra layers at LOCs 6, 7, and 8, respectively (Figs. 2 and 3), with oxidized scoria as the only juvenile component (Fig. 2k). Unlike the LD, juveniles from the PD were apparently aphyric (phenocryst-poor). Lithics in Pagerkandang and Merdada are fresh (dark to grey in color, most of them display porphyritic textures), whereas most of the lithics in the Pangonan have been intensively altered to a yellowish-white colour.

4. Methods

Samples from the lava and pyroclastic domains (LD and PD, respectively) were collected from random and accessible locations. For the pyroclastic deposits (which consisted of several layers), sampling was started from the lower layer to avoid contamination from the upper layer (Suhendro et al. 2021). The pyroclastic samples were sieved manually (-6ϕ (>32 mm) to 3 ϕ (1/8 mm)). Next, we identified and counted all of the grains from -6ϕ to -2ϕ (>32 to 4 mm) sieves to obtain the componentry data.

Based on qualitative traits, we found that each eruptive unit consisted of homogeneous juvenile materials (i.e., lava and scoria). Therefore, each unit is represented by only one thin section. In particular, 14 thin sections (six lava domes, five lava flows, and three scoria clasts) from each unit were observed for petro-graphic analysis to obtain the modal mineralogy and

phenocryst content (ϕ_{PC}). First, all of the observed phenocrysts (from each thin section studied) were manually traced using Corel Draw X7. Second, each resultant image was processed using image-J (i.e., Suhendro et al., 2021, 2022) to obtain the total number and area of the measured phenocrysts. Finally, the vesicle-free phenocryst content was obtained from the following equation (Suhendro et al., 2021):

$$\phi_{PC} = \frac{\sum_{n=1}^{N} A_{PC}}{(A_S - \sum_{n=1}^{N} A_V)} \qquad (1)$$

where $\sum_{n=1}^{N} A_{PC}$ is the total phenocryst area, A_S is sample area in the thin section, and $\sum_{n=1}^{N} A_V$ is the total vesicle area.

Table 1. Glass chemical compositions of scoria clasts. All major elements are shown in weight percent (wt. %). Because scoria clasts are aphanitic, such glass compositions might not differ with the bulk-rock chemical compositions, in agreement to Harijoko et al. (2016).

	LOC 6 (n=5)	LOC 7 (n=5)	LOC 8 (n=5)
SiO_2	56.7	56.9	57.0
Al_2O_3	18.1	18.4	17.8
MgO	4.0	3.9	4.0
CaO	5.9	5.5	5.4
TiO_2	3.1	3.1	3.1
Fe_2O_3	7.9	7.8	7.7
K_2O	2.3	2.4	2.6
Na_2O	1.9	2.0	2.0
Total	99.9	99.9	99.7

The glass chemical compositions of the scoria clasts (Table 1) were determined by scanning electron microscope (SEM) at the Lembaga Pusat Penelitian dan Pengembangan Teknologi Universitas Gadjah Mada (LPPT-UGM), Yogyakarta, Indonesia, using point analysis with a focused beam current of 3 μm (diameter) and an accelerating voltage of 15 kV. As the LD samples were typically dense and lacked vesicles, our textural analysis of the vesicles included only five scoria clasts from PD (Merdada=2, Pagerkandang=2, Pangonan=1). Because the fragmentation process of a phreatomagmatic eruption involves an external agent (i.e., water), a modification of vesicle textures might ha ve occurred. Therefore, the observed scoria clasts were selected from a layer which was interpreted to be of magmatic origin (PF6-1 and PF6 for Merdada, PF7-3(a) and PF 7-5 for Pagerkandang, and PF8-1 for Pangonan).

Vesicles seen at 500x image magnification were manually traced using a Corel Draw X7. Similar to the petrographic analysis, each resultant image was processed using imageJ to obtain the total number and area of the measured vesicles. Finally, the bulk-vesicularity (ϕ_V) and vesicle number density (VND) were obtained using the following equations (Suhendro et al. 2021, 2022):

$$\phi_V = \frac{\sum_{n=1}^{N} A_V}{(A_S - \sum_{n=1}^{N} A_{PC})} \qquad (2)$$

$$VND\ (N_V) = \frac{(\frac{N_a}{d})}{(1 - \phi_V)} \qquad (3)$$

where $\sum_{n=1}^{N} A_V$ is the total vesicle area, A_S is sample area in the thin section, and $\sum_{n=1}^{N} A_{PC}$ is the total phenocryst area, N_a is the number of vesicles per unit area, and d is the average vesicle diameter. Vesicles from 500x image magnification were manually traced using a Corel Draw X7.

5. Results and discussions

5.1 Magmatic source

Based on the petrography, it was found that the PD and LD displayed significant differences in mineralogical content and phenocryst content (Fig. 4). In particular, the scoria clasts from the PD are typically phenocryst poor (3–4 % ϕ_{PC}) and comprise only plagioclase, pyroxene, and oxides as the main phenocryst phase, while lava samples are characteristically phenocryst rich (21–47 % ϕ_{PC}) and includes hydrous minerals (biotite and amphibole) other than plagioclase, pyroxene, and oxides. This distinctive petrographic characteristic suggests that both domains were sourced from different magmatic bodies, where the presence of hydrous minerals represents a lower temperature and more silicic magma composition, and vice versa (McBirney 2007; Ridolfi and Renzulli 2012). This idea was confirmed by the fact that the PD and LD have different bulk-rock chemical compositions (andesite for PD, and andesite-dacite for LD; Harijoko et al., 2016).
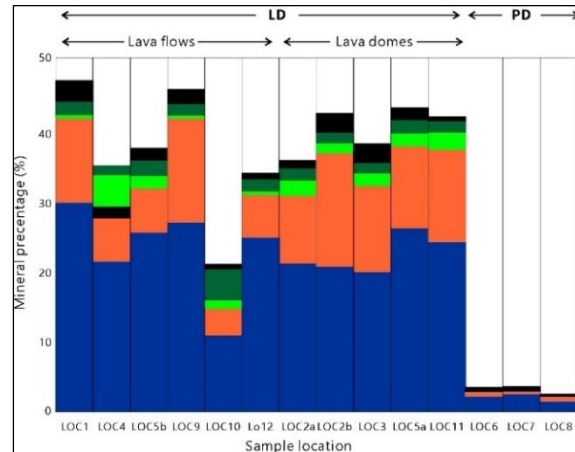
Fig. 4. Diagram showing the fractions of each phenocryst phase in lava domain (LD) and pyroclastic domain (PD). Blue: plagioclase, orange: pyroxene, light green: biotite, dark green: amphibole, black: oxides. Note the significant differences in phenocryst content and mineralogical variations between LD and PD.

5.2 Eruption mechanisms: magmatic or hydromagmatic?

Based on the median size (Md_ϕ) and relative skewness, we found that deposits from PD volcanoes can be grouped into two regimes: (1) coarse-dominated (>2 mm Md_ϕ, positive skewness) and (2) fine-dominated (<2 mm Md_ϕ, negative skewness) (Figs. 3 and 5). Interestingly, the coarse-dominated regime tended to be scoria-rich, whereas the fine-dominated regime was typically lithic-rich.

A scoria (and also pumice) is believed to represent the juvenile phase (primary product of magma fragmentation); hence, its domination may imply that the eruption was magmatic with no and/or minor contribution from external factor such as water. On the other hand, a lithic represents a non-juvenile phase from preexisting rocks; hence, its domination may suggest that the eruption lacked the contribution from primary magma fragmentation. Moreover, it is known that the grain size distribution can be used to depict eruption processes (fragmentation, transport, and deposition) (Jutzeler, Proussevitch, and Allen 2012; Walker 1971; Wohletz, Sheridan, and Brown 1989), where finer grain sizes result in a higher fragmentation index and vice versa (Wohletz and Heiken, 1992). Therefore, we suggest that a coarse- (positive skewness) and scoria-dominated regime was likely produced from a magmatic eruption (Figs. 5 and 6), while a fine- (negative skewness) and lithic-dominated regime was likely produced from phreatomagmatic and/or phreatic eruptions (depending on the presence or absence of juvenile clasts) (Figs. 5 and 6).

The magmatic deposits from Pangonan (PF8-1) have comparatively higher lithic contents compared to those of Merdada and Pagerkandang which might result from an

external factor, that is, alteration. This process may change all of the original rock-forming minerals into clay and ultimately reduce the rock strength (Heap et al., 2021, Lowell and Guilbert, 1970). Consequently, the ascending magmas can easily erode the conduit wall (even though the fragmentation index is low, such as in magmatic eruptions), producing lithic-rich magmatic-fall deposits. The fact that the lithics in Pangonan predominantly consist of altered types does not rule out this possibility (Figs. 3 and 5). When the conduit became larger and surpassed the threshold value of a buoyant plume, the eruption starts to generate PDCs (Suhendro et al., 2021, Wilson et al., 1980) (Fig. 6). As the formation of lava flows and/or domes do not show any association with pyroclastic deposits, it can be inferred that the lava domain (LD) originates from a 'dry' (magmatic) eruption.
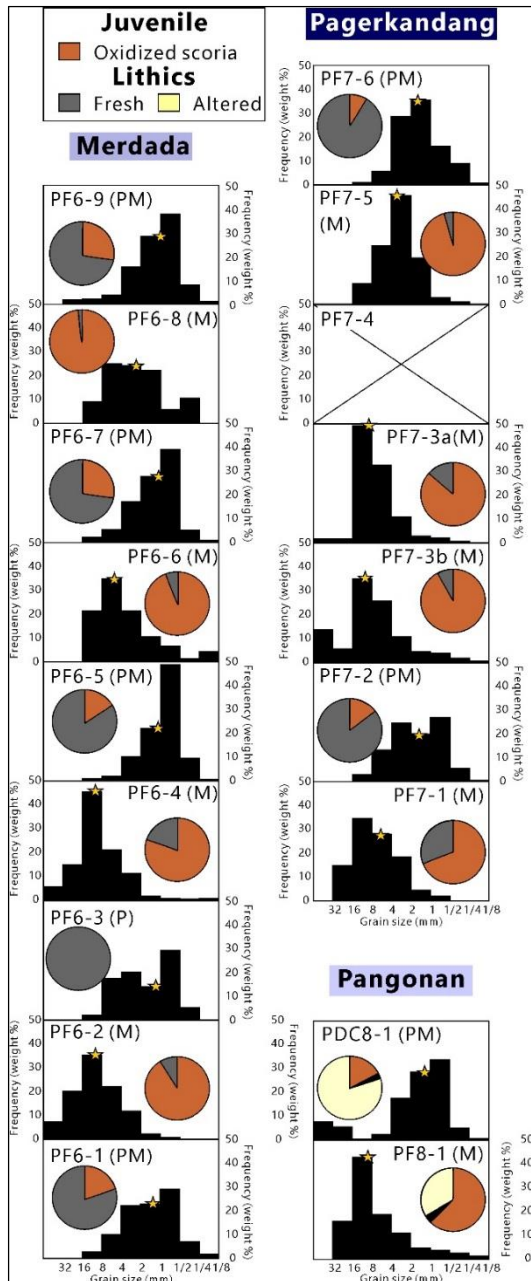
Fig. 5. Histograms and pie-charts showing the grain size distributions (GSDs) and componentry data from Merdada, Pagerkandang, and Pangonan. Star symbol represents median grain size. Note that coarse-dominated layers are scoria-rich and positively skewed, whereas fine-dominated layers are lithic-rich and negatively skewed. M, PM, and P abbreviations are magmatic, phreatomagmatic, and phreatic eruptions, respectively.
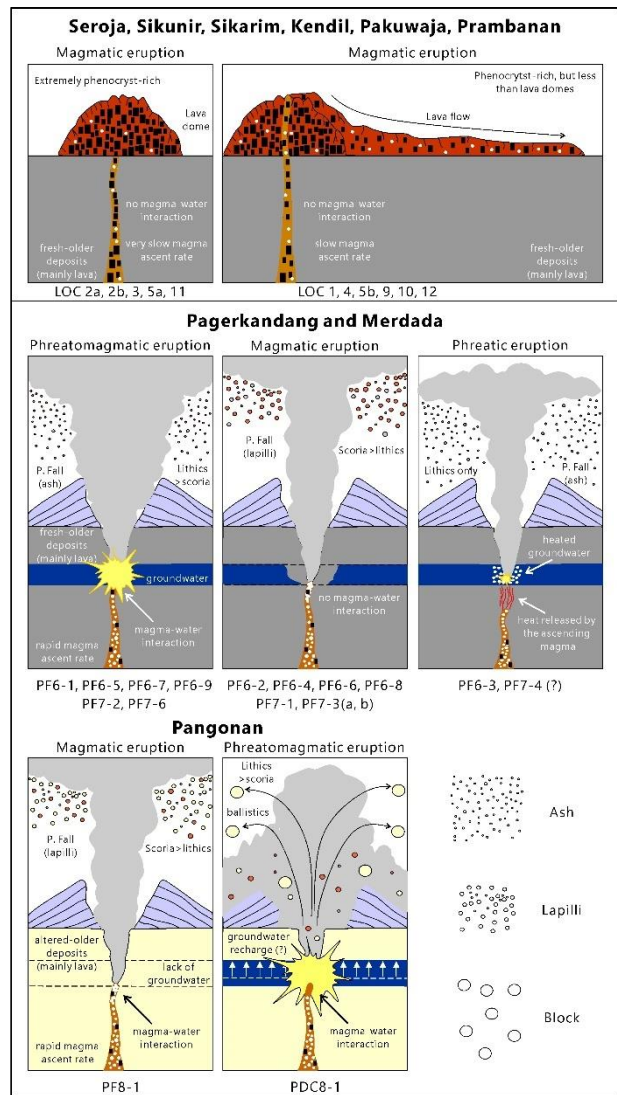
Fig. 6. Cartoon showing the formation process of LD (upper) and PD (lower). In case of LD, the final morphology of lava (flows or domes) seems to depend on the phenocryst abundance. In case of PD, the eruption mechanisms (magmatic, phreatomagmatic, or phreatic) have strong dependence on the contact ratio between magma and water.

5.3 The role of bubbles (observed as vesicles in the pyroclasts) in an ascending magma

Vesicles are fossil gases in magmas that act as the main driving force for volcanic eruptions (Toramaru 2006). Therefore, quantifying the number density may provide some clues on the degree of explosivity and magma decompression rate (a higher VND represents a more energetic and faster magma ascent rate and vice versa; Shea, 2017, Toramaru, 2006). However, it is important to note that vesicles in an effusive product (e.g., lava) are not representative of VND measurements as they have experienced intense modification (bubble expansion and coalescence) due to the very slow magma ascent rate.

Based on the aforementioned idea, we can assume that the PD results from an explosive eruption due to the presence of moderately vesicular (27–41 % ϕ_V) and high VNDs ($1.1 \times 10^5 mm^{-3}$ - $4.9 \times 10^5 mm^{-3}$) scoria clasts (Fig. 7). Such VND values were found to be higher than those of pyroclastic cone-producing eruptions (i.e., Ichulbong, South Korea and Black point, USA) (Fig. 7) due to the difference in silica compositions (Pangonan, Merdada, and Pagerkandang are andesitic, whereas Ichulbong and Black point are basaltic; Murtagh et al., 2011,

Murtagh and White, 2013) and the magma decompression rates (a higher magma decompression rate results in a higher VND; Toramaru, 2006). Such an explosive manner becomes the main reason why the crater sizes of the PD volcanoes are typically large (4.3×10^5-8.9×10^5 m^2) (Fig. 1b). On the other hand, the LD must originate in an effusive manner because the main eruptive products are lava domes and/or flows. This is the main reason why the LD has characteristically small crater sizes (0.1×10^5-1.5×10^5 m^2) (Fig. 1b). Moreover, our petrographic data (Fig. 3) also show that lava dome samples typically have higher phenocryst content than the lava flows (avg. ϕ_{PC} of 40 % and 36 %, respectively). This implies that a more phenocryst-rich magma tends to produce a lava dome because of its higher effective viscosity, whereas less phenocryst magmas imply a lower effective magma viscosity, thus forming lava flow.
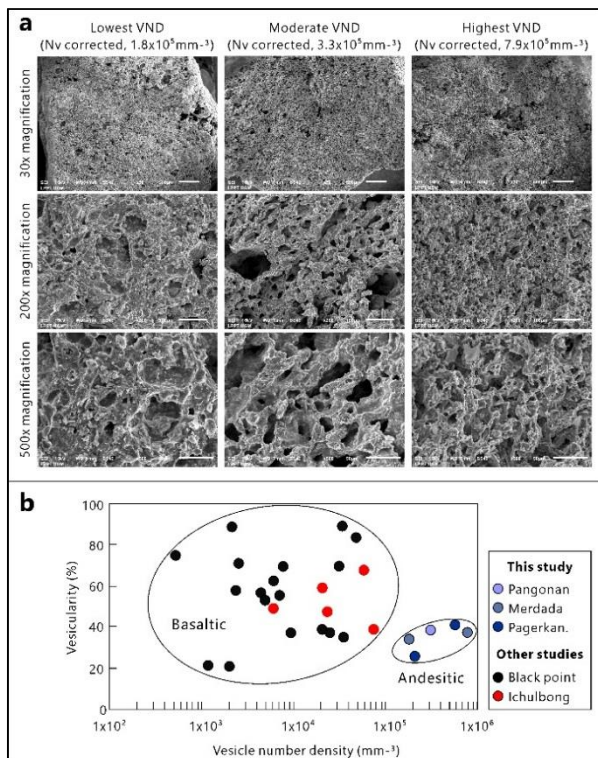
Fig. 7. (a) Representative vesicle images of scoria clasts erupted from pyroclastic domain (PD) volcanoes. Scale bars correspond to 500, 100, and 50 microns for 30x, 200x, and 500x image magnifications, respectively. (b) Comparison between VND and vesicularity values of PD volcanoes (this study) with Ichulbang and Black point.

5.4. Possible hazards

As discussed in the previous sub-sections, the LD and PD form under different eruption manners, that is, effusive and explosive, respectively. This implies that the S-SE and N-NW sectors have different volcanic styles. In particular, the LD tends to produce "dry" and weak (qualitatively very low VND) magmatic eruptions, making lava flows and/or domes the main volcanic hazard that threatens civilization settlements in the S-SE sector. On the other hand, the formation of the PD includes an intercalation between explosive magmatic, phreatomagmatic, and phreatic eruptions. Most of hydromagmatic eruptions occur in the W-NW sector because of the existence of a geothermal system beneath Pagerkandang, Merdada, and Pangonan (Harijoko et al. 2016). Consequently, such dynamic conditions make the prediction of future eruption styles becomes difficult. We pointed out that the W-SW sector is facing the major threat from ballistics, fallout material (ash and lapilli), and highly destructive PDCs.

6. Conclusions

We identified the possible hazards that might occur in the Dieng volcanic complex (DVC) by identifying the rock characteristics of the DVC post-caldera volcanoes. The domination of pyroclastic materials (mostly lapilli and ash, with scoria as the juvenile phase) in pyroclastic domain (PD) suggest that the civilizations in W-SW sector are facing major threat from an explosive magmatic-phreatomagmatic-phreatic eruptions. By contrast, lava domain (LD) is dominated by lava flows and/or domes, suggesting that a weak (effusive) magmatic eruption is the major threat in S-SE sector.

References

Araya, Naoki, Michihiko Nakamura, Atsushi Yasuda, Satoshi Okumura, Tomoki Sato, Masato Iguchi, Daisuke Miki, and Nobuo Geshi. 2019. Shallow Magma Pre-Charge during Repeated Plinian Eruptions at Sakurajima Volcano. *Scientific Reports* 9(1). doi: 10.1038/s41598-019-38494-x.

Badan Pusat Statistik Kabupaten Wonosobo. 2020. Proyeksi Penduduk Desa Di Kecamatan Kejajar (access time: July 4, 2022, 12:46 am).

Browne, Brandon L., Christina Neal, and Charles R. Bacon. 2022. *THE ~400 YR B.P. ERUPTION OF HALF CONE, A POST-CALDERA COMPOSITE CONE WITHIN ANIAKCHAK CALDERA, ALASKA PENINSULA*.

le Guern, F., H. Tazieff, and R. Faivre Pierret. 1982. *An Example of Health Hazard: People Killed by Gas during a Phreatic Eruption: Dieng Plateau (Java, Indonesia), February 20th 1979*.

Harijoko, Agung, Ryusuke Uruma, Haryo Edi Wibowo, Lucas Doni Setijadji, Akira Imai, Kotaro Yonezu, and Koichiro Watanabe. 2016. Geochronology and Magmatic Evolution of the Dieng Volcanic Complex, Central Java, Indonesia and Their Relationships to Geothermal Resources. *Journal of Volcanology and Geothermal Research* 310:209–24. doi: 10.1016/j.jvolgeores.2015.12.010.

Heap, Michael J., Tobias Baumann, H. Albert Gilg, Stephan Kolzenburg, Amy G. Ryan, Marlène Villeneuve, J. Kelly Russell, Lori A. Kennedy, Marina Rosas-Carbajal, and Michael A. Clynne. 2021. Hydrothermal Alteration Can Result in Pore Pressurization and Volcano Instability. *Geology* 49(11):1348–52. doi: 10.1130/G49063.1.

Jutzeler, M., A. A. Proussevitch, and S. R. Allen. 2012. Grain-Size Distribution of Volcaniclastic Rocks 1: A New Technique Based on Functional Stereology. *Journal of Volcanology and Geothermal Research* 239–240:1–11. doi: 10.1016/j.jvolgeores.2012.05.013.

Lowell JD, and Guilbert JM. 1970. Lateral and Vertical Alteration-Mineralization Zoning in Porphyry Ore Deposits. *Economic Geology* 65:373–408.

McBirney, AR. 2007. *Igneous Petrology*. Third. Jones and Bartlett Publisher, USA.

Murtagh, Rachel M., and James D. L. White. 2013. Pyroclast Characteristics of a Subaqueous to Emergent Surtseyan Eruption, Black Point Volcano, California. *Journal of Volcanology and Geothermal Research* 267:75–91. doi: 10.1016/j.jvolgeores.2013.08.015.

Murtagh, Rachel M., James D. L. White, and Young Kwan Sohn. 2011. Pyroclast Textures of the Ilchulbong 'wet'

Tuff Cone, Jeju Island, South Korea. *Journal of Volcanology and Geothermal Research* 201(1–4):385–96. doi: 10.1016/j.jvolgeores.2010.09.009.

Rachmat, Heryadi, Mega Fatimah Rosana, A. Djumarma Wirakusumah, and Gamma Abdul Jabbar. 2016. Petrogenesis of Rinjani Post-1257-Caldera-Forming-Eruption Lava Flows. *Indonesian Journal on Geoscience* 3(2):107–26. doi: 10.17014/ijog.3.2.107-126.

Reubi, O., and I. A. Nicholls. 2004. Variability in Eruptive Dynamics Associated with Caldera Collapse: An Example from Two Successive Eruptions at Batur Volcanic Field, Bali, Indonesia. *Bulletin of Volcanology* 66(2):134–48. doi: 10.1007/s00445-003-0298-6.

Ridolfi, Filippo, and Alberto Renzulli. 2012. Calcic Amphiboles in Calc-Alkaline and Alkaline Magmas: Thermobarometric and Chemometric Empirical Equations Valid up to 1,130°C and 2.2 GPa. *Contributions to Mineralogy and Petrology* 163(5):877–95. doi: 10.1007/s00410-011-0704-6.

Rubin', K. H., G. E. Wheller, O. Tanzer, J. D. Macdougall, R. Varne, and R. Finkel. 1989. *238U Decay Series Systematics of Young Lavas from Batur Volcano, Sunda Arc*. Vol. 38.

Shea, Thomas. 2017. Bubble Nucleation in Magmas: A Dominantly Heterogeneous Process? *Journal of Volcanology and Geothermal Research* 343:155–70.

Sigurdsson H. 2000. *Encyclopedia of Volcanoes*. Academic Press.

Suhendro I. 2016. "Karakteristik Batuan Hasil Erupsi Gunung Api Dalam Kaldera (Intrar Caldera) Ijen, Desa Kalianyar, Kecamatan Sempol, Kabupaten Bondowoso." Universitas Gadjah Mada, Yogyakarta.

Suhendro, Indranova, Atsushi Toramaru, Agung Harijoko, and Haryo Edi Wibowo. 2022. The Origins of Transparent and Non-Transparent White Pumice: A Case Study of the 52 Ka Maninjau Caldera-Forming Eruption, Indonesia. *Journal of Volcanology and Geothermal Research* 431. doi: 10.1016/j.jvolgeores.2022.107643.

Suhendro, Indranova, Atsushi Toramaru, Tomoharu Miyamoto, Yasuo Miyabuchi, and Takahiro Yamamoto. 2021. Magma Chamber Stratification of the 1815 Tambora Caldera-Forming Eruption. *Bulletin of Volcanology* 83(10). doi: 10.1007/s00445-021-01484-x.

Sukhyar R, Sumartadipura NS, and Effendi W. 1986. "Peta Geologi Komplek Gunungapi Dieng."

Toramaru, A. 2006. BND (Bubble Number Density) Decompression Rate Meter for Explosive Volcanic Eruptions. *Journal of Volcanology and Geothermal Research* 154(3–4):303–16. doi: 10.1016/j.jvolgeores.2006.03.027.

Walker, George P. L. 1971. Grain-Size Characteristics of Pyroclastic Deposits. *The Journal of Geology* 79(6): 696-714.

Wilson, Lionel, R. Stephen J. Sparks, and George P. L. Walker. 1980. Explosive Volcanic Eruptions — IV. The Control of Magma Properties and Conduit Geometry on Eruption Column Behaviour. *Geophysical Journal of the Royal Astronomical Society* 63(1):117–48. doi: 10.1111/j.1365-246X.1980.tb02613.x.

Wohletz, K. H., M. F. Sheridan, and W. K. Brown. 1989. Particle Size Distributions and the Sequential Fragmentation/Transport Theory Applied to Volcanic Ash. *Journal of Geophysical Research* 94(B11). doi: 10.1029/jb094ib11p15703.

Wohletz KH, and Heiken G. 1992. *Volcanology and Geothermal Energy*. University of California Press, USA.